

EUROPEAN ORGANIZATION FOR NUCLEAR RESEARCH

CERN-EP/81-125
8 October 1981

MEASUREMENT OF ($D^+\bar{D}$) CHARM-MESON PAIR PRODUCTION

IN (pp) INTERACTIONS AT $\sqrt{s} = 62$ GeV

M. Basile, G. Cara Romeo, L. Cifarelli, A. Contin, G. D'Ali,
P. Di Cesare, B. Esposito, P. Giusti, T. Massam, R. Nania,
F. Palmonari, G. Sartorelli, G. Valenti and A. Zichichi

CERN, Geneva, Switzerland

Istituto di Fisica dell'Università, Bologna, Italy

Istituto di Fisica dell'Università, Perugia, Italy

Istituto Nazionale di Fisica Nucleare, Bologna, Italy

Istituto Nazionale di Fisica Nucleare, LNF, Frascati, Italy

ABSTRACT

The charm meson D^+ is observed in (pp) interactions at 62 GeV centre-of-mass energy, in association with its antimeson, D^- or \bar{D}^0 . The cross-section for ($D^+\bar{D}$) pair production is evaluated according to various hypotheses on the production mechanisms. The value of the cross-section is found to be $\sim 300 \mu\text{b}$ when both the D^+ and the \bar{D} are assumed to be "centrally" produced.

(Submitted to Nuovo Cimento)

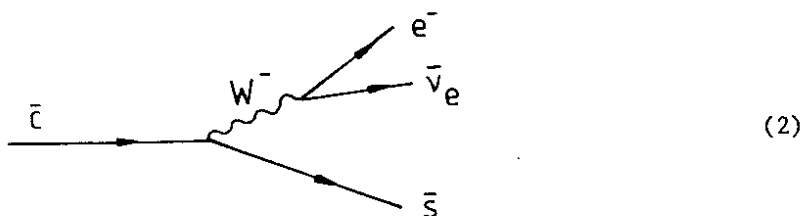
1. INTRODUCTION

The associated production of charm-meson pairs ($D^+\bar{D}$) in high-energy (pp) interactions is reported.

The D^+ was detected via its hadronic decay mode,

$$D^+ \rightarrow K^- \pi^+ \pi^+ , \quad (1)$$

whilst the presence of the associated antimeson, either D^- or \bar{D}^0 , was signalled by the identification of its semileptonic decay, which follows the Cabibbo-dominant antiquark transition:



Hence the reactions studied were

$$pp \rightarrow D^+ + e^- + \text{anything} , \quad (3)$$

and

$$pp \rightarrow D^+ + (e^- K^+) + \text{anything} . \quad (4)$$

The e^- or the $(e^- K^+)$ system in the final state were used as "signatures" of the anticharm semileptonic decay.

The results of the observation of a D^+ signal in reactions (3) and (4) are given in Sections 2 and 3, respectively. In Section 4, the cross-section for ($D^+\bar{D}$) pair production is estimated, according to various hypotheses on the production mechanisms. The conclusions are presented in Section 5.

2. ANALYSIS WITH THE e^- TRIGGER OF THE $(K^- \pi^+ \pi^+)$ MASS SPECTRUM

The experimental apparatus was installed at the Split-Field Magnet (SFM) intersection of the CERN Intersecting Storage Rings (ISR). It consisted of a multi-wire proportional chamber (MWPC) system for track reconstruction and momentum measurement, and of auxiliary detectors:

- i) to select electrons or positrons at 90° (electromagnetic shower detectors, gas threshold Čerenkov counters, and a "dE/dx" chamber);
- ii) to achieve some hadron identification up to ~ 2 GeV/c momentum (time-of-flight counters, TOF).

We refer the reader elsewhere¹⁻⁴⁾ for details on the various parts of the apparatus, including the electron (positron) filter and the hadron identification procedure.

The data were collected at $\sqrt{s} = 62$ GeV, by triggering on a minimum energy release ($E_{\min} \gtrsim 500$ MeV) in the electromagnetic shower counters. The number of triggered events was $\sim 3 \times 10^6$ and corresponded to an integrated luminosity $\mathcal{L} \simeq 4.4 \times 10^{36} \text{ cm}^{-2}$.

In order to study reaction (3), the $(K^- \pi^+ \pi^+)$ invariant mass spectrum was analysed for those events where an e^- was detected.

The selection criteria were the following:

- i) the identification of an e^- with a transverse momentum $p_T \geq 0.5$ GeV/c;
- ii) the identification of a K^- via the time-of-flight technique (K_{TOF}^-), which implied the K momentum to be below 1.5 GeV/c;
- iii) the presence of two positive pions defined as any two particles having $|x_L| < 0.3$ *), and not identified by TOF as positive kaons or protons (the latter was a loose condition since the TOF hodoscope covered only $\sim 10\%$ of the solid angle).

Each of the above tracks was required to originate from the reconstructed event vertex within ± 5 cm and to have a momentum measured with less than 30% uncertainty. The uncertainty in the e^- case was required to be less than 15%.

*) Below $|x_L| = 0.3$, the contamination from "leading" protons can be neglected⁵⁾.

The $(K_{\text{TOF}}^- \pi^+ \pi^+)$ mass spectrum, obtained in coincidence with an e^- , is shown in Fig. 1. A small enhancement is observed, in the D^+ mass range, of (29 ± 15) mass combinations.

The background mass distribution was derived by the "event mixing" method. This consisted in taking a K_{TOF}^- from one e^- triggered event, and combining this K_{TOF}^- with a $(\pi^+ \pi^+)$ pair from the next event. The open circles in Fig. 1 are the results of this "event mixing" method.

Following the expectation of a rather high- p_T production for the heavy D^+ meson^{*}), we have applied to the data the condition

$$p_T(K_{\text{TOF}}^- \pi^+ \pi^+) \geq 0.7 \text{ GeV}/c .$$

The resulting invariant mass plot is shown in Fig. 2. Here a more significant D^+ peak shows up, with (39 ± 11) mass combinations corresponding to about 3.5 standard deviations. The ratio events/combinations in the peak is 0.6.

The "event mixing" background (open circles) is reported in Fig. 2: its shape agrees well with that of the spectrum where the D^+ peak emerges. Notice the improvement in the "signal-to-background" ratio between the data of Figs. 1 and 2.

The D^+ peak is not present in e^+ triggered events (see Fig. 3). In fact, as specified earlier, the associated production of $(D^+ \bar{D})$ pairs can only occur when an e^- , not an e^+ , appears in the final state.

The events obtained with the e^- trigger and with the condition $p_T \geq 0.7 \text{ GeV}/c$ have been analysed in terms of a possible resonant contribution to the D^+ decay:



In the $(K_{\text{TOF}}^- \pi^+ \pi^+)$ mass spectrum, we defined an "in" region (i.e. where the D^+ is observed) and two "out" regions (i.e. below and above the D^+ peak, each as wide as the "in" region). For the events falling into the "in" and "out" regions,

^{*}) We have measured the p_T dependence of the D^+ to be $\exp(-2.3 p_T)$, as will be reported elsewhere⁶⁾.

respectively, we have plotted the $(K_{\text{TOF}}^- \pi^+)$ invariant mass spectra. The results are shown in Figs. 4a and 4b. In these figures the data with the e^- trigger are compared with those obtained with the "wrong" trigger, e^+ . A small excess of (11 ± 5) combinations is found in the \bar{K}^{*0} mass range, for the "in" case only (Fig. 4a).

By doing the reverse, i.e. by requiring the $(K_{\text{TOF}}^- \pi^+)$ mass to be in the \bar{K}^{*0} region, the D^+ peak in the $(K_{\text{TOF}}^- \pi^+ \pi^+)$ mass distribution (shown in Fig. 5) is in turn reduced to (12 ± 5) mass combinations. The "signal-to-background" ratio is, however, improved with respect to that of Fig. 2. Notice that the background distribution superimposed in Fig. 5 is obtained by repeating the same analysis on e^+ triggered events, i.e. using the "wrong" trigger.

With the above data we obtain the branching ratio value:

$$\frac{D^+ \rightarrow \bar{K}^{*0} \pi^+}{D^+ \rightarrow K^- \pi^+ \pi^+} = 0.31 \pm 0.16 ,$$

in agreement with existing measurements^{7,8)}.

3. ANALYSIS WITH THE $(e^- K_{\text{TOF}}^+)$ TRIGGER OF THE $(K^- \pi^+ \pi^+)$ MASS SPECTRUM

A more selective trigger for the antimeson decay was the requirement of both an e^- and a K_{TOF}^+ in the final state, according to diagram (2). Such a requirement had already been successfully applied in the same experiment to the search for the neutral D^0 charmed meson, decaying into $(K^- \pi^+)$, produced in association with its antimeson⁹⁾.

Reaction (4) was studied, with the following conditions:

- i) for the "trigger" to consist of an e^- (selected as in Section 2) plus a K^+ , identified by the TOF system, i.e. K_{TOF}^+ ;
- ii) for the $(K^- \pi^+ \pi^+)$ final state to consist of any negative particle not identified as π^- or \bar{p} in the TOF hodoscope, and of two positive particles having the same characteristics as in Section 2.

The $(K^-\pi^+\pi^+)$ invariant mass system was then derived for the $(e^-K_{TOF}^+)$ triggered events. However, further requirements were imposed in order to reduce the combinatorial background, which was obviously higher than in the $(K_{TOF}^-\pi^+\pi^+)$ case. These conditions are listed below:

- i) $p_T(K^-\pi^+\pi^+) \geq 0.4 \text{ GeV}/c$;
- ii) $|y(K^-\pi^+\pi^+)| < 1.5$ (where $y = (1/2) \ln [(E+p_L)/(E-p_L)]$ is the rapidity);
- iii) $|\Delta\phi(e^-,K_{TOF}^+)| < 90^\circ$ (where ϕ is the azimuthal angle around the beam axis and $\Delta\phi$ is the angular difference between the e^- and the K_{TOF}^+).

Conditions (i) and (ii) were suggested by the fact that a high- p_T ⁶⁾ and a "central"¹⁰⁾ production mechanism are expected for a charm meson; condition (iii) implied a "same-side" angular correlation between the decay products of the anti-meson*).

The $(K^-\pi^+\pi^+)$ invariant mass distribution ensuing from this analysis is plotted in Fig. 6. A D^+ signal with (33 ± 9) mass combinations, corresponding to about 3.5 standard deviations, is again observed.

To verify that the $(e^-K_{TOF}^+)$ trigger was indeed due to the anticharm semileptonic decay, we have used data with a "wrong" anticharm trigger, i.e. $(e^+K_{TOF}^+)$, where the e^+ has the wrong charge. The result is shown in Fig. 7, where there is no evidence for any effect in the $(K^-\pi^+\pi^+)$ mass spectrum.

It should be mentioned that the two sets of events selected in Sections 2 and 3, respectively, are independent. In fact Section 2 required K_{TOF}^- , whilst Section 3 required K_{TOF}^+ , and the number of events containing a $(K_{TOF}^+K_{TOF}^-)$ pair was negligible.

*) Such a correlation had already been observed in the D^0 case. For the $(e^-K_{TOF}^+)$ triggered events giving at least one $(K^-\pi^+)$ combination in the D^0 peak, the ratio $[(e^-K_{TOF}^+)_{\text{same side}}/(e^-K_{TOF}^+)_{\text{opposite side}}]$ was measured to be (1.5 ± 0.2) . For those falling below and above the peak, the ratio was (1.1 ± 0.1) .

4. CROSS-SECTION ESTIMATES

In order to evaluate the ($D^+\bar{D}$) pair cross-section, some assumptions are needed. The inclusive production mechanisms of the D^+ and the \bar{D} mesons can be described according to models. We have chosen, for consistency, those formerly used for the associated charm production of ($A_c^+\bar{D}$) and ($D^0\bar{D}$), observed in the same experiment^{9,11}).

These models are based on the following production distributions:

- i) "central" production: $E(d^3\sigma/dp^3) \sim (1 - |x_L|)^a \exp(-bp_T)$,
- ii) "flat-y" production: $E(d^3\sigma/dp^3) \sim \exp(-bp_T)$ (i.e. $d\sigma/d|y| = \text{const}$),
- iii) "flat- x_L " production: $d^3\sigma/dp^3 \sim \exp(-bp_T)$ (i.e. $d\sigma/d|x_L| = \text{const}$),

where $a = 3$, $b = 2$ (GeV/c)⁻¹, and y and x_L are the already quoted rapidity and longitudinal fractional momentum, respectively.

The associated ($D^+\bar{D}$) production was assumed to occur via different combinations of the above three distributions. Moreover, the two mesons were supposed to be produced in an uncorrelated way. The semileptonic decay of the antimeson was described by a K_{e3} -like matrix element. The acceptance of the apparatus, corresponding to each production model, was calculated by Monte Carlo simulation.

For the cross-section estimates, we have limited our Monte Carlo simulations to reaction (3). The results relative to reaction (4) will be reported in a subsequent paper¹²).

The detection efficiencies for the e^- and the K_{TOF}^- in reaction (3), obtained via Monte Carlo, turned out to be $\sim 45\%$ and $\sim 65\%$, respectively.

The decay branching ratios were taken to be^{8,13})

- i) for decay (1):

$$\frac{D^+ \rightarrow K^- \pi^+ \pi^+}{D^+ \rightarrow \text{all}} = 0.063 \pm 0.015 ,$$

- ii) for decay (2):

$$\frac{\bar{D} \rightarrow e^- + \text{anything}}{\bar{D} \rightarrow \text{all}} = 0.085 \pm 0.015 .$$

The results are summarized in Table 1, where the cross-section estimates have an over-all error of $\sim 50\%$.

5. CONCLUSIONS

The production of $(D^+\bar{D})$ charmed-meson pairs in high-energy (pp) interactions at $\sqrt{s} = 62$ GeV in the (pp) centre-of-mass system has been reported.

The presence of the antimeson was guaranteed by the identification of either an e^- or both an e^- and a K^+ from its semileptonic decay. The associated D^+ meson was detected by means of the hadronic three-body decay $D^+ \rightarrow K^-\pi^+\pi^+$.

The resonant decay $D^+ \rightarrow \bar{K}^{*0}\pi^+ \rightarrow K^-\pi^+\pi^+$ has been observed.

The total cross-section estimates agree, within the large errors, with those relative to $(D^0\bar{D})$ pair production, measured in the same experiment⁹⁾. The hypothesis where both the D^+ and the \bar{D} mesons are produced "centrally" corresponds to the smallest cross-section value, as was the case for $(D^0\bar{D})$ pairs.

However, the value of $\sigma_{\text{central}}(D^+\bar{D}) \sim 300 \mu\text{b}$ suggests, once again, that charm is more copiously produced in high-energy hadronic interactions than was so far theoretically expected in the framework of perturbative QCD¹⁴⁾.

REFERENCES

- 1) M. Basile, G. Cara Romeo, L. Cifarelli, A. Contin, G. D'Ali, P. Di Cesare, B. Esposito, L. Favale, P. Giusti, T. Massam, F. Palmonari, G. Sartorelli, G. Valenti and A. Zichichi, Nucl. Instrum. Methods 179, 477 (1981).
- 2) H. Frehse, F. Lapique, M. Panter and F. Piuz, Nucl. Instrum. Methods 156, 87 (1978).
H. Frehse, M. Heiden, M. Panter and F. Piuz, Nucl. Instrum. Methods 156, 97 (1978).
- 3) M. Basile, G. Cara Romeo, L. Cifarelli, A. Contin, G. D'Ali, P. Giusti, T. Massam, F. Palmonari, G. Sartorelli, G. Valenti and A. Zichichi, Nucl. Instrum. Methods 163, 93 (1979).
- 4) M. Basile, G. Cara Romeo, L. Cifarelli, A. Contin, G. D'Ali, P. Di Cesare, B. Esposito, P. Giusti, T. Massam, F. Palmonari, G. Sartorelli, G. Valenti and A. Zichichi, A measurement of the prompt e^{\pm} production cross-section in proton-proton collisions at $\sqrt{s} = 62$ GeV, preprint CERN-EP/81-92 (1981), and Nuovo Cimento, in press.
- 5) P. Capiluppi, G. Giacomelli, A.M. Rossi, G. Vannini, A. Bertin, A. Bussièrè and E.J. Ellis, Nucl. Phys. B79, 189 (1974).
- 6) M. Basile, G. Cara Romeo, L. Cifarelli, A. Contin, G. D'Ali, P. Di Cesare, B. Esposito, P. Giusti, T. Massam, R. Nania, F. Palmonari, G. Sartorelli, G. Valenti and A. Zichichi, The p_T dependence of charmed mesons produced in (pp) interactions at $\sqrt{s} = 62$ GeV, preprint CERN-EP/81-127 (1981), and Nuovo Cimento Letters, in press.
- 7) D. Drijard, H.G. Fischer, W. Geist, R. Gokieli, P.G. Innocenti, V. Korbèl, A. Minten, A. Norton, R. Sosnowski, S. Stein, O. Ullaland, H.D. Wahl, P. Burland, M. Della Negra, G. Fontaine, P. Fzenkiel, C. Ghesquière, D. Linglin, G. Sajot, H. Frehse, E.E. Kluge, M. Heiden, A. Putzer, J. Stiewe, P. Hanke, W. Hofman, M. Panter, K. Rauschnabel, J. Spengler and D. Wegener, Phys. Lett. 81B, 250 (1979).

- A. Putzer, Report given at the Discussion Meeting between Experimentalists and Theorists on ISR and Collider Physics (eds. M.G. Albrow and M. Jacob, Series 2, No. 4 (April 1981), p. 5.
- 8) R. H. Schindler, M.S. Alam, A.M. Boyarski, M. Breidenbach, D.L. Burke, J. Dorenbosch, J.M. Dorfan, G.J. Feldman, M.E.B. Franklin, G. Hanson, K.G. Hayes, T. Himel, D.G. Hitlin, R.J. Hollebeek, W.R. Innes, J.A. Jaros, P. Jenni, R.R. Larsen, V. Lüth, M.L. Perl, B. Richter, A. Roussarie, D.L. Scharre, R.F. Schwitters, J.L. Siegrist, H. Taureg, M. Tonutti, R.A. Vidal, J.M. Weiss and H. Zacccone; G. Abrams, C.A. Blocker, A. Blondel, W.C. Carithers, W. Chinowsky, M.W. Coles, S. Cooper, W.E. Dieterle, J.B. Dillon, M.W. Eaton, G. Gidal, G. Goldhaber, A.D. Johnson, J.A. Kadyk, A.J. Lankford, R.E. Millikan, M.E. Nelson, C.Y. Pang, J.F. Patrick, J. Strait, G.H. Trilling, E.N. Vella and I. Videau, Phys. Rev. D 24, 78 (1981), and references therein.
- 9) M. Basile, G. Cara Romeo, L. Cifarelli, A. Contin, G. D'Ali, P. Di Cesare, B. Esposito, P. Giusti, T. Massam, R. Nania, F. Palmonari, G. Sartorelli, G. Valenti and A. Zichichi, Measurement of associated production of ($D^0\bar{D}$) in (pp) interactions at $\sqrt{s} = 62$ GeV, preprint CERN-EP/81-73 and Nuovo Cimento Letters, in press.
- 10) M. Basile, G. Cara Romeo, L. Cifarelli, A. Contin, G. D'Ali, P. Di Cesare, B. Esposito, P. Giusti, T. Massam, R. Nania, F. Palmonari, G. Sartorelli, G. Valenti and A. Zichichi, The longitudinal momentum distribution of charm mesons produced in (pp) interactions at $\sqrt{s} = 62$ GeV, preprint CERN EP/81-126 (1981), and Nuovo Cimento Letters, in press.
- 11) M. Basile, G. Cara Romeo, L. Cifarelli, A. Contin, G. D'Ali, P. Di Cesare, B. Esposito, P. Giusti, T. Massam, F. Palmonari, G. Sartorelli, G. Valenti, and A. Zichichi, Nuovo Cimento 63A, 230 (1981).

- 12) M. Basile, G. Cara Romeo, L. Cifarelli, A. Contin, G. D'Ali, P. Di Cesare, B. Esposito, P. Giusti, T. Massam, R. Nania, F. Palmonari, G. Sartorelli, G. Valenti and A. Zichichi, Cross-section estimates for $pp \rightarrow (D^+ \rightarrow K^- \pi^+ \pi^+) + (\bar{D} \rightarrow e^- K^+ X) + \text{anything}$ at $\sqrt{s} = 62$ GeV and (x_L, p_T) distributions, in preparation.
- 13) J.M. Feller, A.M. Litke, R.J. Madaras, M.T. Ronan, A. Barbaro-Galtieri, J.M. Dorfan, R. Ely, G.J. Feldman, A. Fong, B. Gobbi, G. Hanson, J.A. Jaros, B.P. Kwan, P. Lecomte, D. Lüke, J.F. Martin, D.H. Miller, S.I. Parker, M.L. Perl, I. Peruzzi, M. Piccolo, T.P. Pun, P.A. Rapidis, R.R. Ross, D.L. Scharre, T.G. Trippe, V. Vuillemin and D.E. Yount, Phys. Rev. Lett. 40, 1677 (1978).
-
- W. Bacino, R. Burns, P. Condon, P. Cowell, A. Diamant-Berger, G. Donaldson, M. Duro, T. Ferguson, A. Hall, G. Irwin, J. Kirkby, J. Kirz, F. Merritt, L. Nodulman, W. Slater, H. Ticho and S. Wojcicki, Phys. Rev. Lett. 43, 1073 (1979), and references therein.
- 14) For a review of experimental results and theoretical predictions, see for instance, F. Muller, Hadroproduction of charmed particles, Invited talk given at the 4th Warsaw Symposium on Elementary Particle Physics, Kazimierz, Poland, May 1981, CERN/EP/0457R/RM/ed (June 1981) and references quoted therein.

Table 1

Cross-section estimates for $(D^+\bar{D})$ pair production
(see Section 4). The uncertainty on the values
reported is $\sim 50\%$.

D^+ production distribution	\bar{D} production distribution	σ_{tot} (μb)
$E \frac{d\sigma}{d x_L } \propto (1 - x_L)^3$	$E \frac{d\sigma}{d x_L } \propto (1 - x_L)^3$	305
$\frac{d\sigma}{d y } = \text{const}$	$\frac{d\sigma}{d y } = \text{const}$	730
$\frac{d\sigma}{d x_L } = \text{const}$	$\frac{d\sigma}{d x_L } = \text{const}$	> 5000
$\frac{d\sigma}{d x_L } = \text{const}$	$E \frac{d\sigma}{d x_L } \propto (1 - x_L)^3$	2035
$E \frac{d\sigma}{d x_L } \propto (1 - x_L)^3$	$\frac{d\sigma}{d x_L } = \text{const}$	1080

Figure captions

- Fig. 1 : $(K_{\text{TOF}}^- \pi^+ \pi^+)$ invariant mass distribution with the e^- trigger. The circles and the dashed-line curve superimposed show the normalized "event mixing" background distribution and fit, respectively.
- Fig. 2 : Same as Fig. 1, with the additional condition $p_T(K_{\text{TOF}}^- \pi^+ \pi^+) \geq 0.7$ GeV/c.
- Fig. 3 : $(K_{\text{TOF}}^- \pi^+ \pi^+)$ invariant mass spectrum obtained with the "wrong" e^+ trigger and $p_T(K_{\text{TOF}}^- \pi^+ \pi^+) \geq 0.7$ GeV/c. The "event mixing" background fit, shown in Fig. 2, is superimposed (dashed line).
- Fig. 4 : $(K_{\text{TOF}}^- \pi^+)$ invariant mass obtained with the e^- trigger for the events falling:
- a) "in" the D^+ peak of the $(K_{\text{TOF}}^- \pi^+ \pi^+)$ spectrum shown in Fig. 2;
 - b) "below" and "above" the D^+ peak.
- The dashed-line background histograms are obtained with the e^+ trigger. The full-line curves are fits to the latter.
- Fig. 5 : $(K_{\text{TOF}}^- \pi^+ \pi^+)$ invariant mass for e^- triggered events when $p_T(K_{\text{TOF}}^- \pi^+ \pi^+) \geq 0.7$ GeV/c and $m(K_{\text{TOF}}^- \pi^+)$ in the K^{0*} mass range. The dashed-line curve is a fit to the same distribution obtained with the e^+ trigger.
- Fig. 6 : $(K^- \pi^+ \pi^+)$ invariant mass spectrum obtained when an $(e^- K_{\text{TOF}}^+)$ trigger is present in the final state. The dashed line, showing the flat background shape, is derived by "event mixing".
- Fig. 7 : $(K^- \pi^+ \pi^+)$ invariant mass spectrum obtained with the "wrong" $(e^+ K_{\text{TOF}}^+)$ trigger. A fit to this spectrum is superimposed as a dashed line.

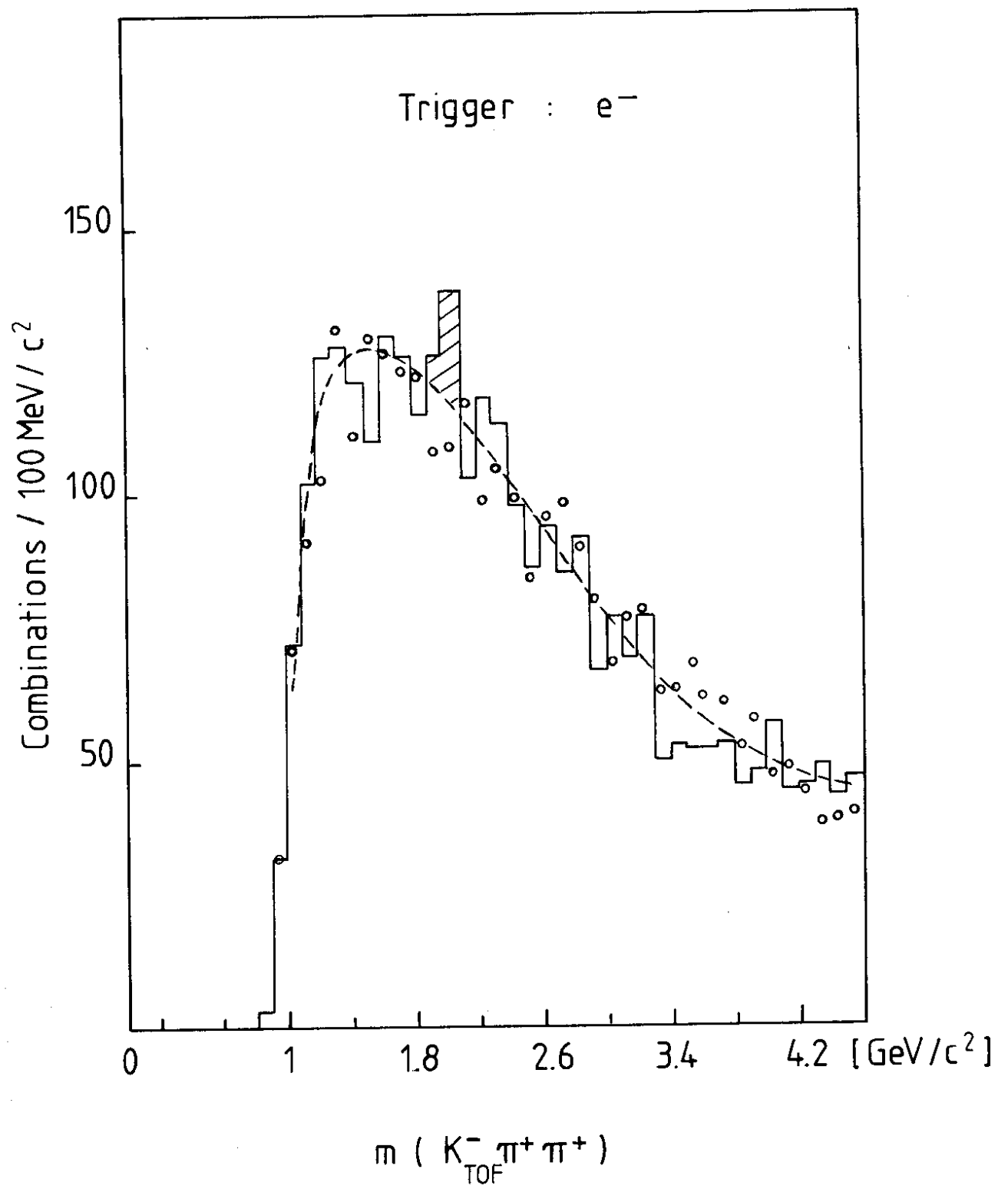


Fig. 1

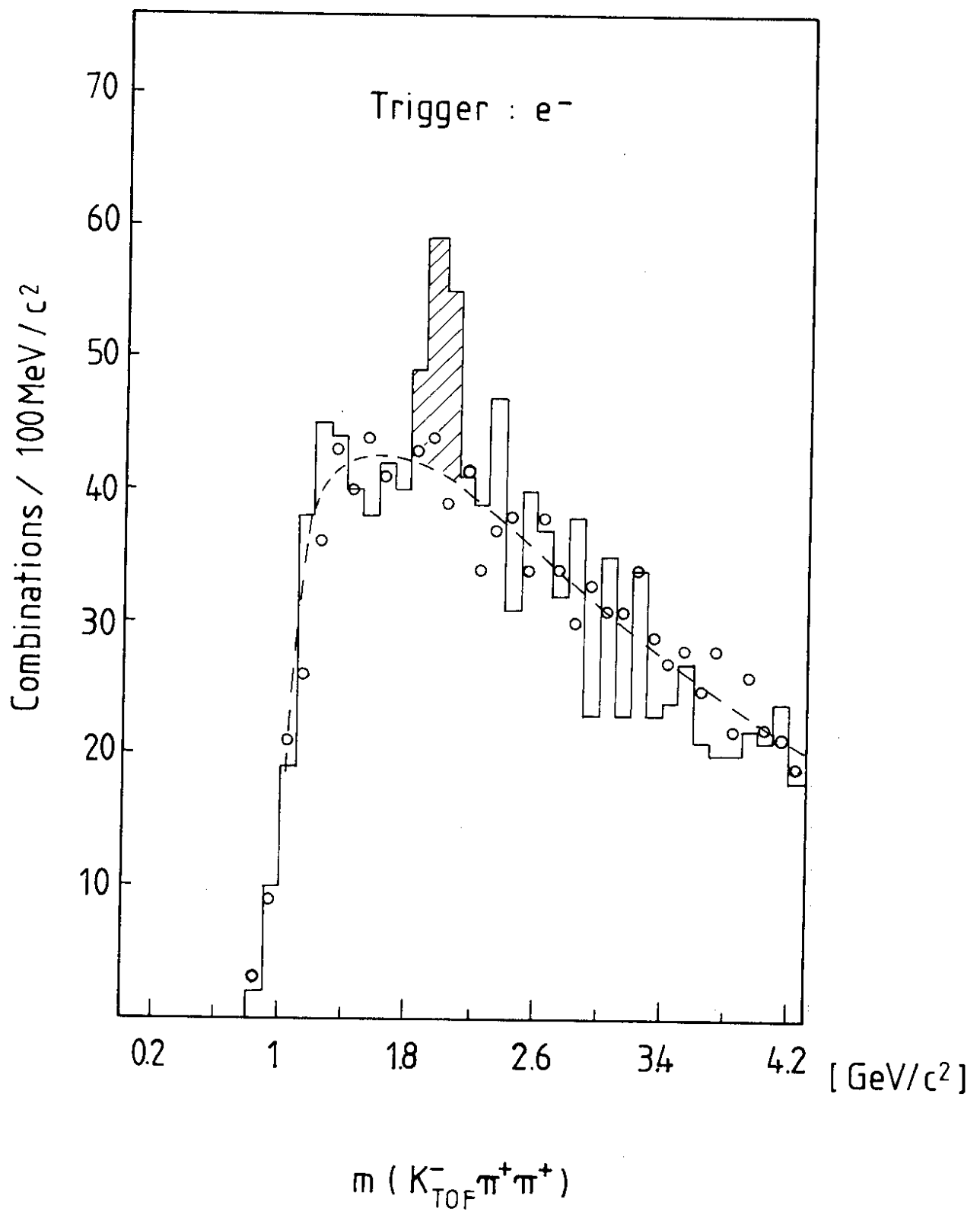


Fig. 2

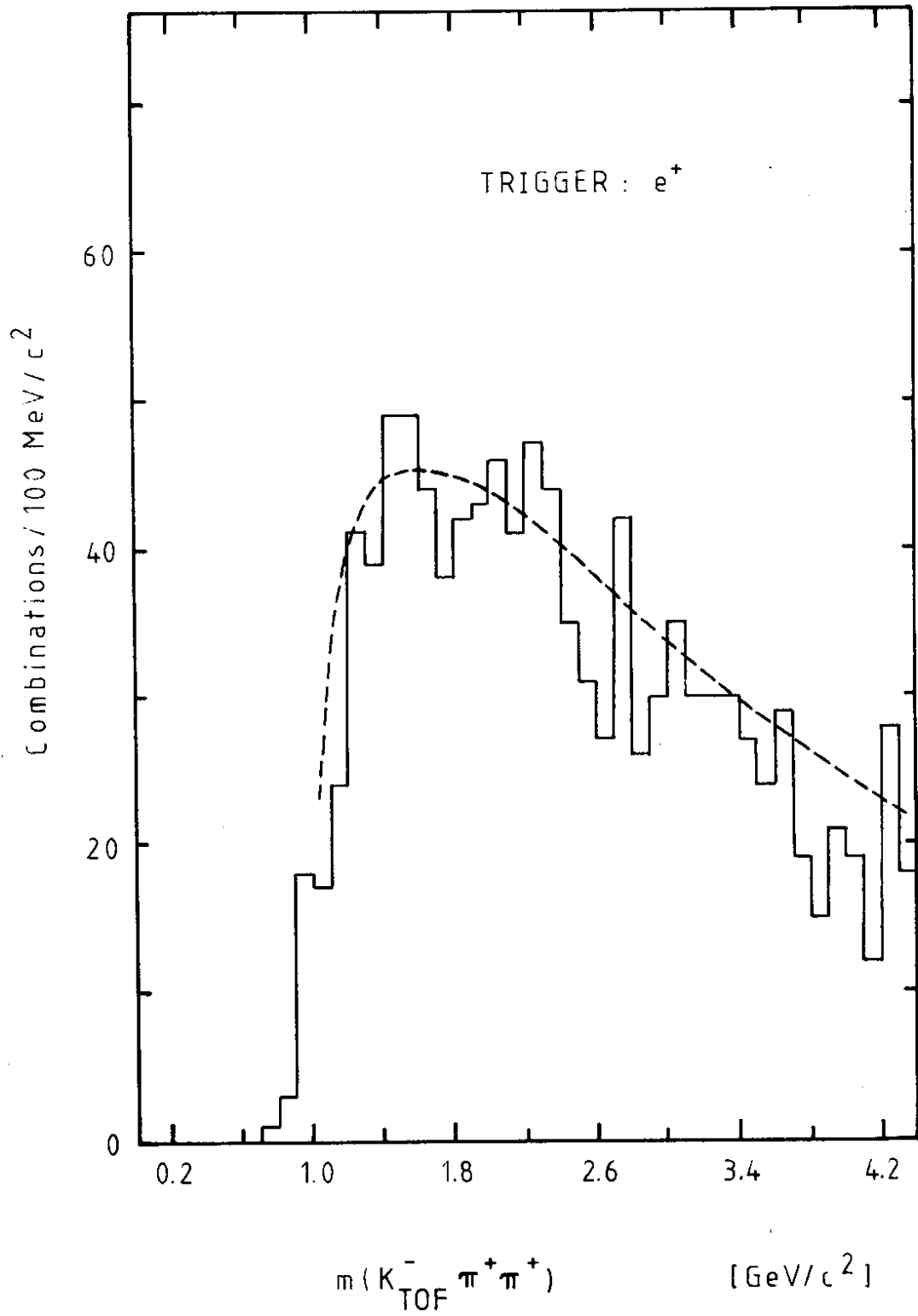


Fig. 3

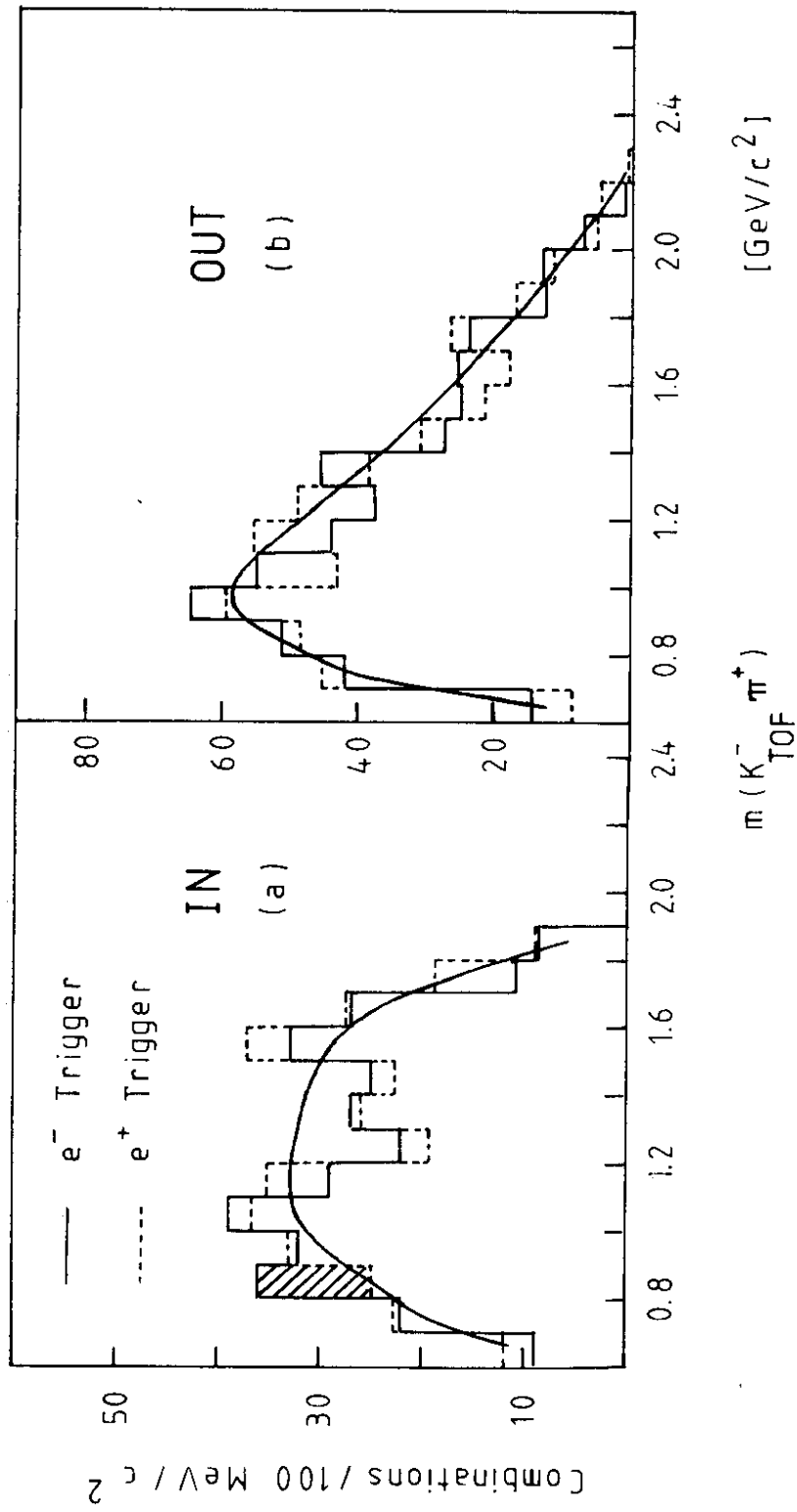


Fig. 4

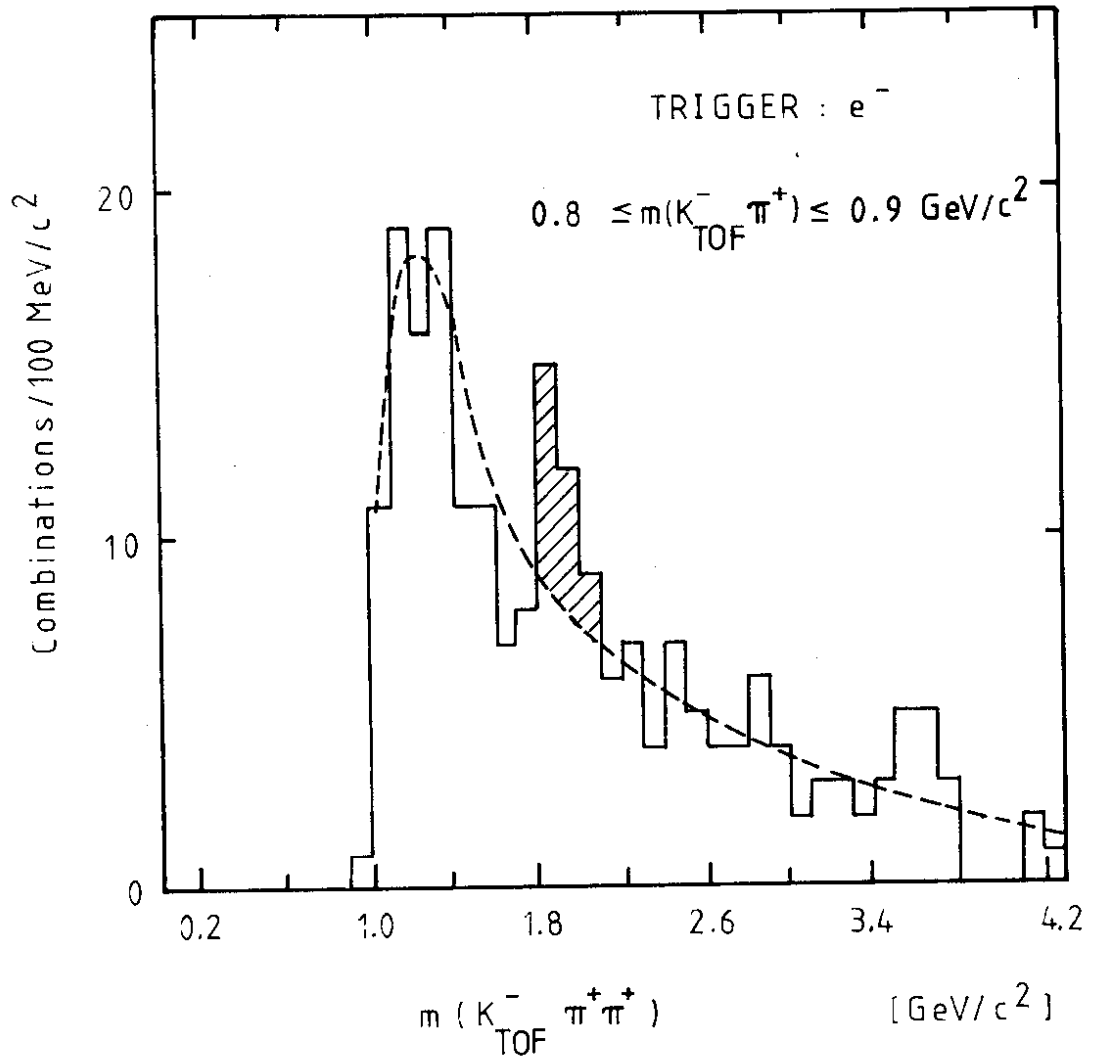


Fig. 5

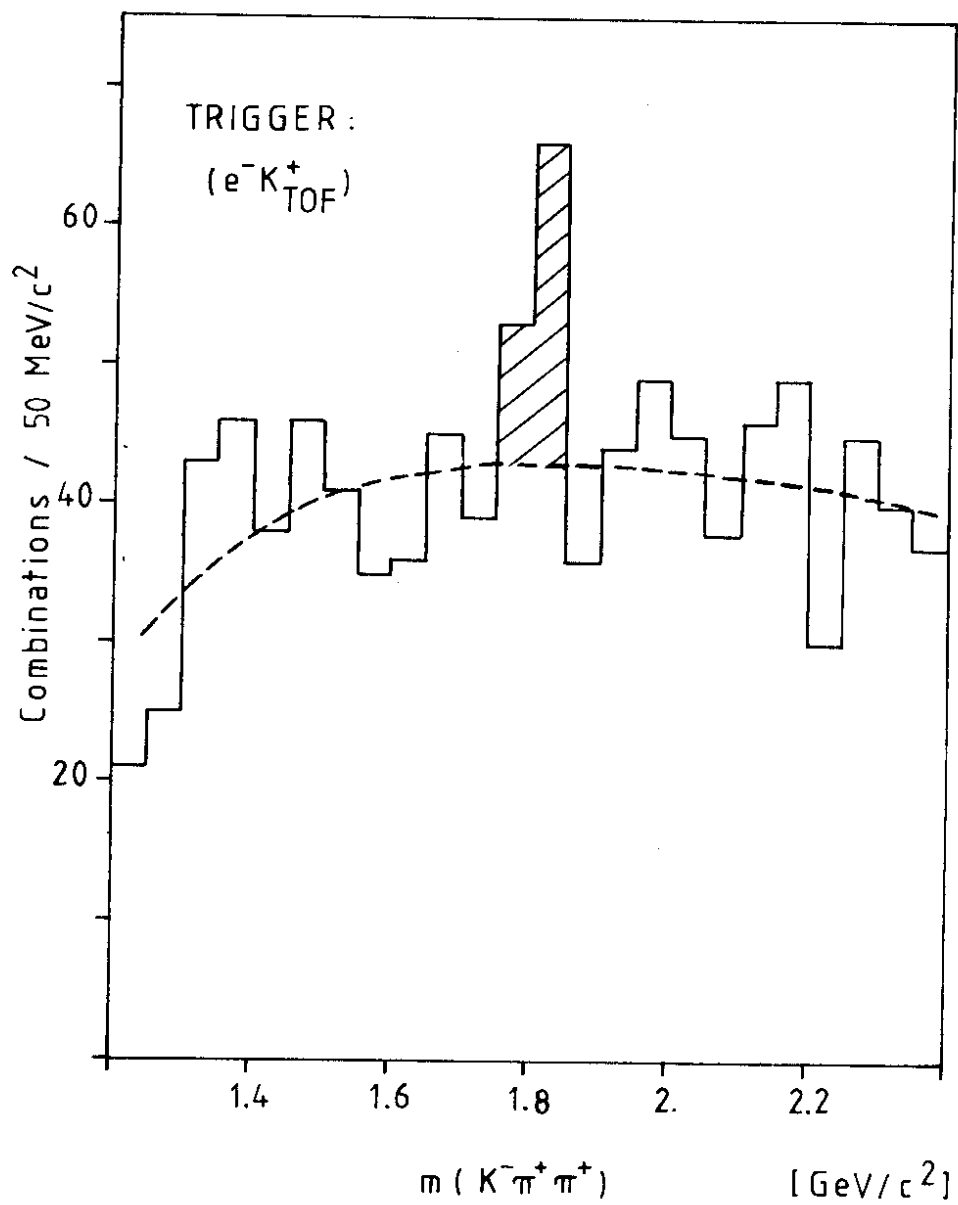


Fig. 6

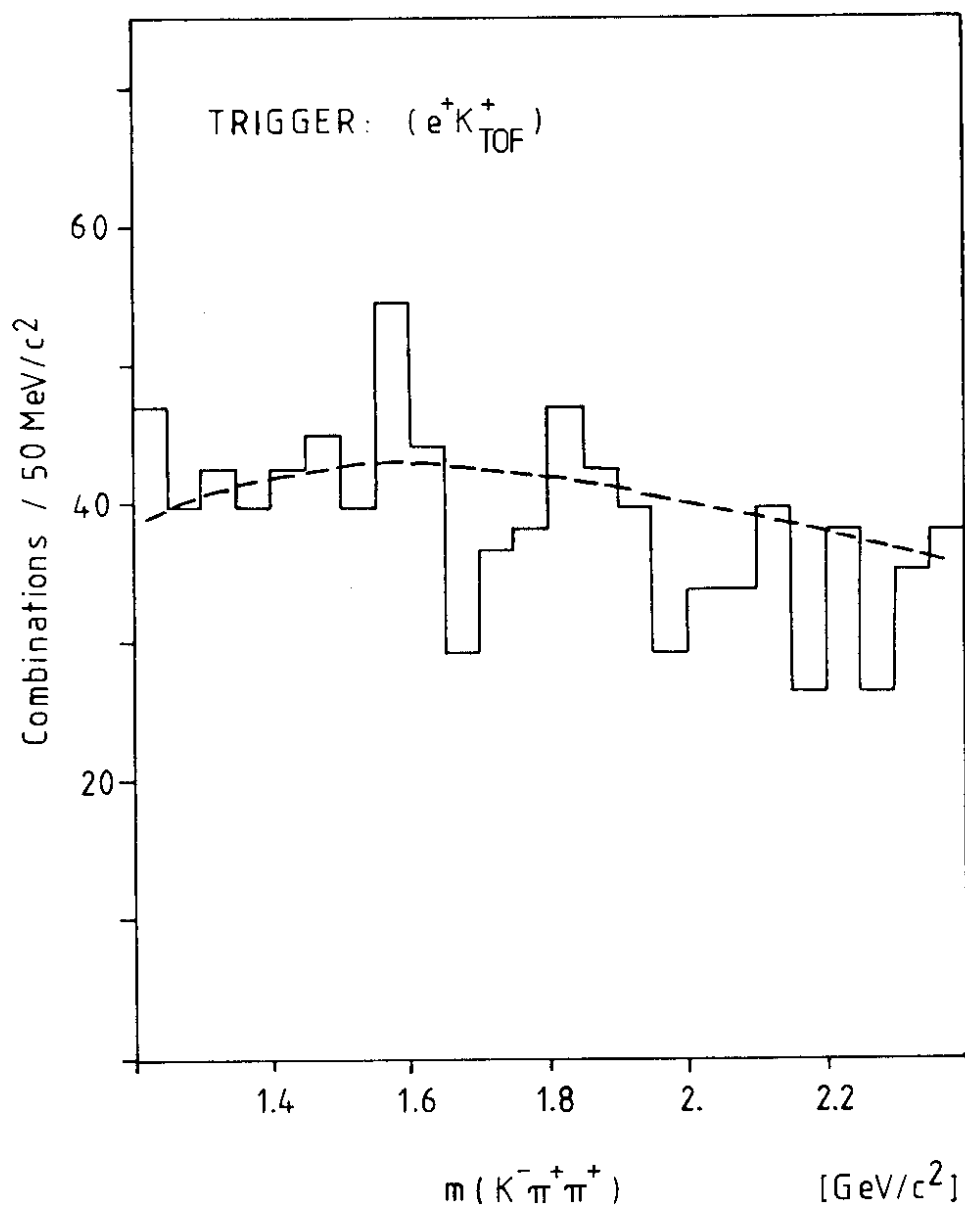


Fig. 7

